



NUMERICAL IMPLEMENTATION OF THE ARBITRARY CRACK FRONT FOR THREE DIMENSIONAL PROBLEMS

EL KABIR Soliman¹, MOUTOU PITTI Rostand^{2,3}, DUBOIS Frederic¹, LAPUSTA
Yuri⁴, RECHO Naman^{2,5},

¹Université de Limoges, Centre du génie Civil, GC2D, 19300 Egletons, France

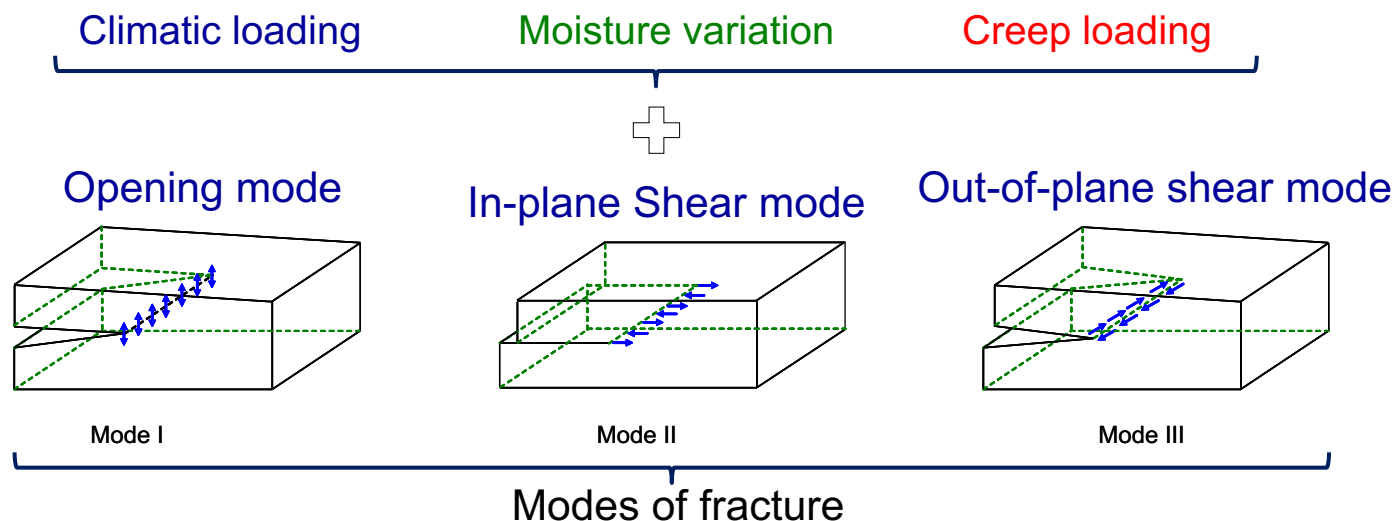
²Université Clermont Auvergne, CNRS, Institut Pascal, F-63000 Clermont-Ferrand, France

³CENAREST, IRT, BP 14070, Libreville, Gabon

⁴SIGMA, Institut Pascal, 63171 Aubière, France

⁵EPF, Engineering school, 2 rue Fernand Sastre, Troyes, France

- Predicting the behavior of structures under mixed mode loading
- Developing specific tools for three-dimensional configurations
- Consider thickness effect under variable environments
- Need for applications related to the inspection and diagnosis of structures

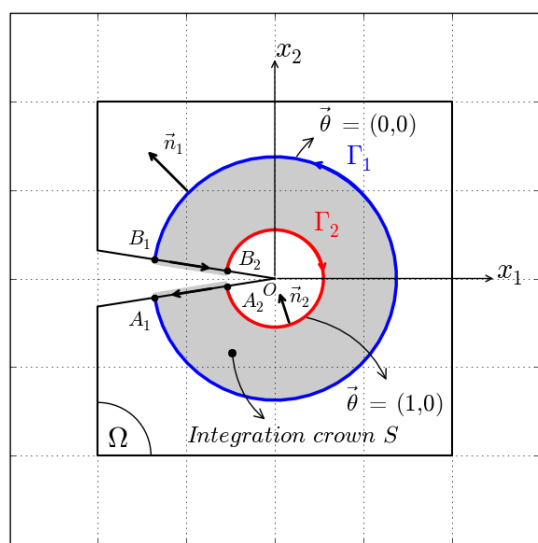


- Scientific context
- Part I : three dimensional contour integral generalizations
 - Analytical formulation (J^{3D} and G_θ^{3D} -integral)
 - Numerical implementation
- Part II : mixed mode three dimensional contour integral
 - Analytical formulation (M_θ^{3D} -integral)
 - Mixed mode Numerical implementation
- Conclusions and outlooks

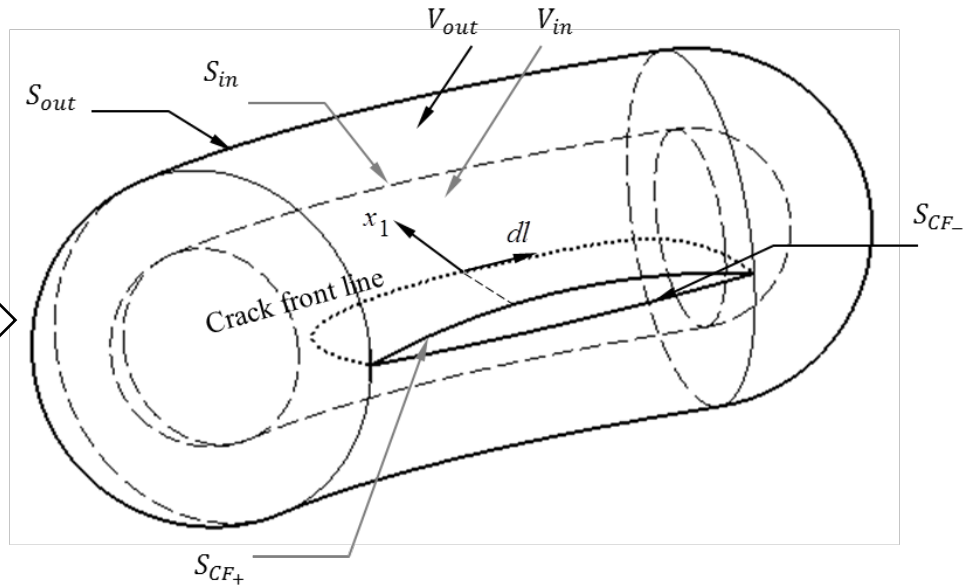
J-integral in 3D configurations

Rice's integral

$$J^{2D} = \int_{\Gamma} \left(W \cdot n_1 - (\sigma_{ij} \cdot n_j \cdot u_{i,1}) \right) \cdot d\Gamma$$



**Integration domain size
for 2D**



**3D Closed volume and
surfaces integration
domains**

The main advance of this form is the presence of an arbitrary crack front line enclosed by a 3D surface



J^{3D} and G_θ^{3D} -integral description

The J-integral formulation is based on the Noether's theorem application (Noether 1918) :

$$\delta L = \int_V \int_t \delta W \cdot dV \cdot dt = 0$$

A Gauss-Ostrogradski transformation allows us writing the Lagrangian's invariance in the form:

$$\int_S \left(W \cdot n_k - (\sigma_{ij} \cdot n_j \cdot u_{i,k}) \right) \cdot dS + \int_V \left(\sigma_{ij} \cdot (\varepsilon_{ij})_{,k} - W_{,k} \right) \cdot dV = 0$$

the J^{3D} -integral is defined as below:

$$J^{3D} = \int_{S_{\Gamma_{out}}} \left(W \cdot n_1 - (\sigma_{ij} \cdot n_j \cdot u_{i,1}) \right) \cdot dS - \int_{S_{cr}} \sigma_{ij} \cdot u_{i,1} \cdot n_j \cdot dS - \int_{V_{\Gamma_{out}}} \left(W_{,1} - \sigma_{ij} \cdot (\varepsilon_{ij})_{,1} \right) \cdot dV$$



Stationary crack



Crack lips pressure



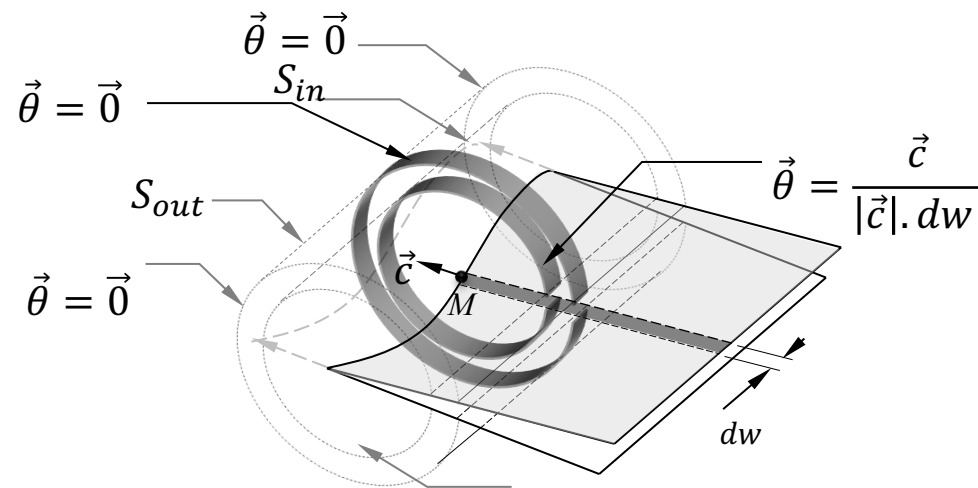
Crack propagation

$$G_\theta = \int_V (P_{kj} \cdot \theta_{k,j}) \cdot n_j \cdot dV + \int_{S_{CF}} \sigma_{ij} \cdot u_{i,k} \cdot n_j \cdot \theta_k \cdot dS - \int_{V_{\Gamma_2}} \left(W_{,k} - \sigma_{ij} \cdot (\varepsilon_{ij})_{,k} \right) \cdot \theta_k \cdot dV$$



$$G_\theta = \int_V (P_{kj} \cdot \theta_{k,j}) \cdot n_j \cdot dV + \int_{S_{CF}} \sigma_{ij} \cdot u_{i,k} \cdot n_j \cdot \theta_k \cdot dS - \int_{V_{\Gamma_2}} \left(W_{,k} - \sigma_{ij} \cdot (\varepsilon_{ij})_{,k} \right) \cdot \theta_k \cdot dV$$

① ② ③



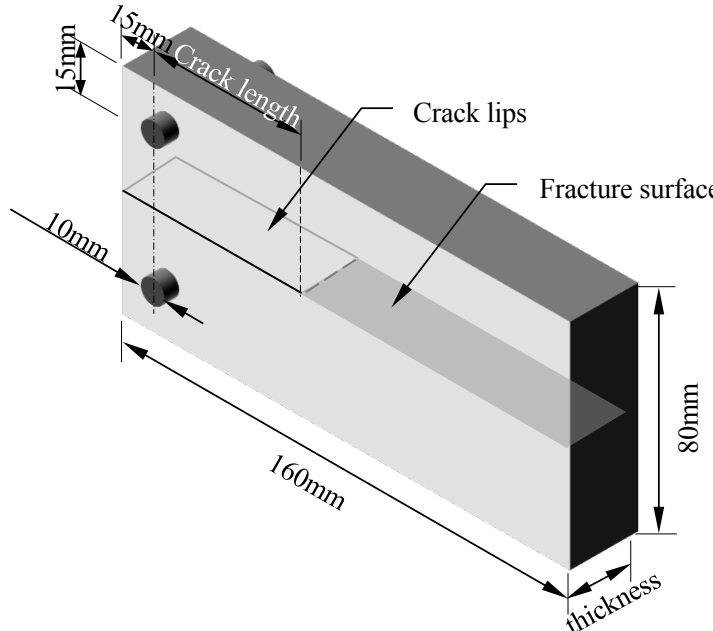
$\vec{\theta} = \vec{0}$

$$\vec{\theta} = 0 \text{ on } S_{\Gamma_{out}}, \vec{\theta} = \frac{\vec{c}}{|\vec{c}| \cdot dw} \text{ on } C \cap S_{\Gamma_{out}} \text{ and } \vec{\theta} = 0 \text{ on } S_{\Gamma_{in}}$$

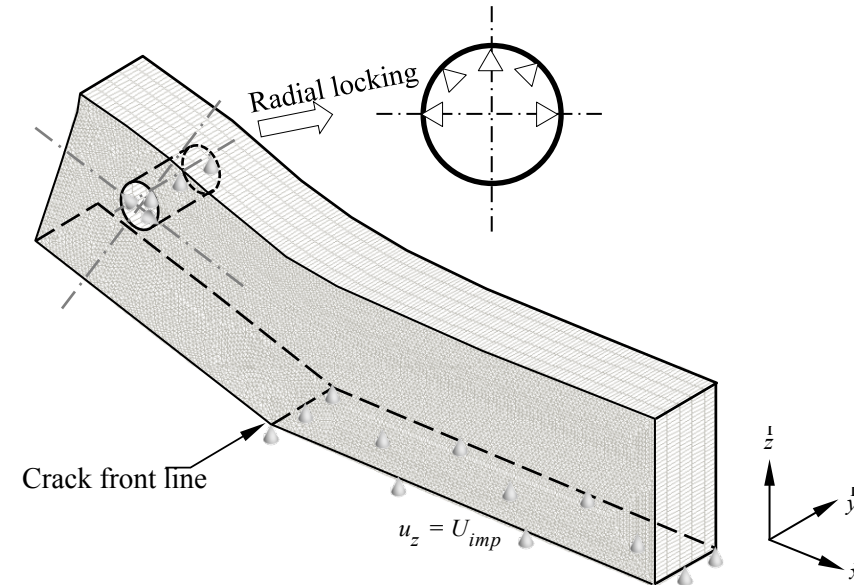
The average energy release rate can be calculated with an integration of along the crack front line divided by the crack width

Numerical validation

The finite element implementation is based on a Double Cantilever Beam loaded in an open mode.

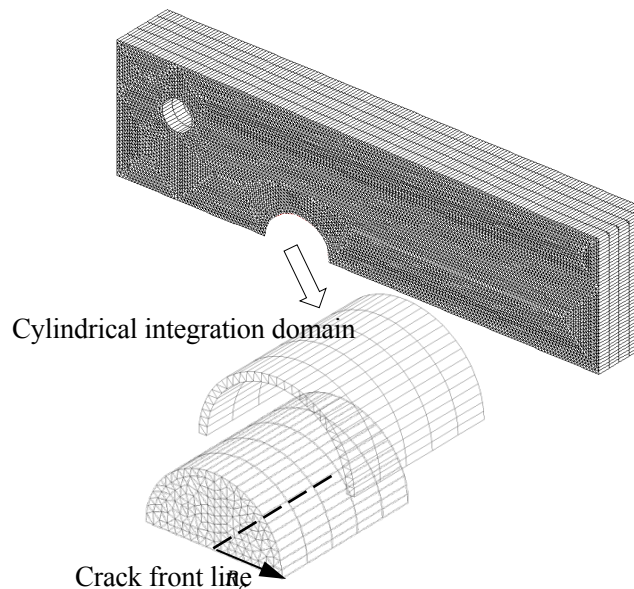


Specimen DCB

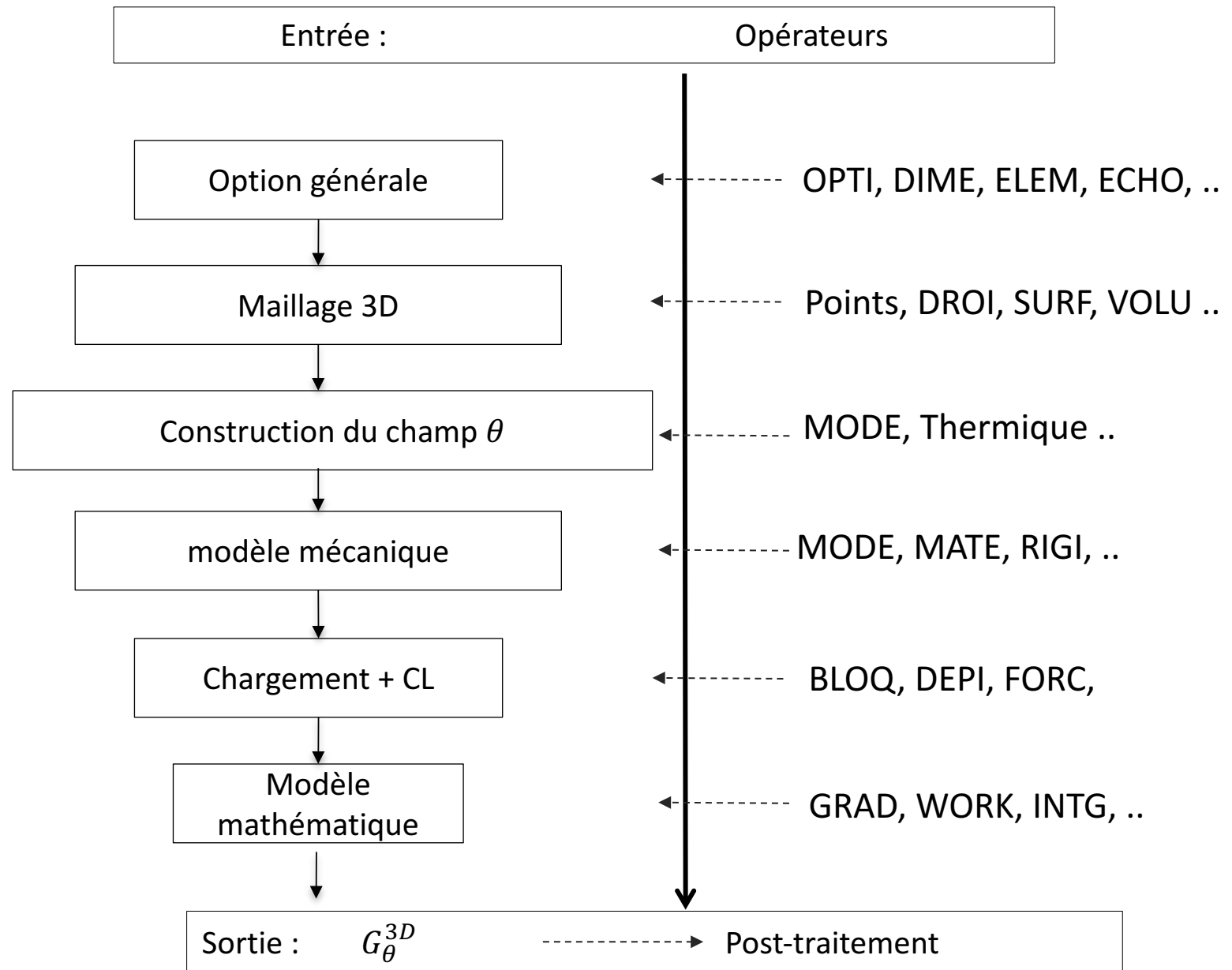


Material is characterized by :

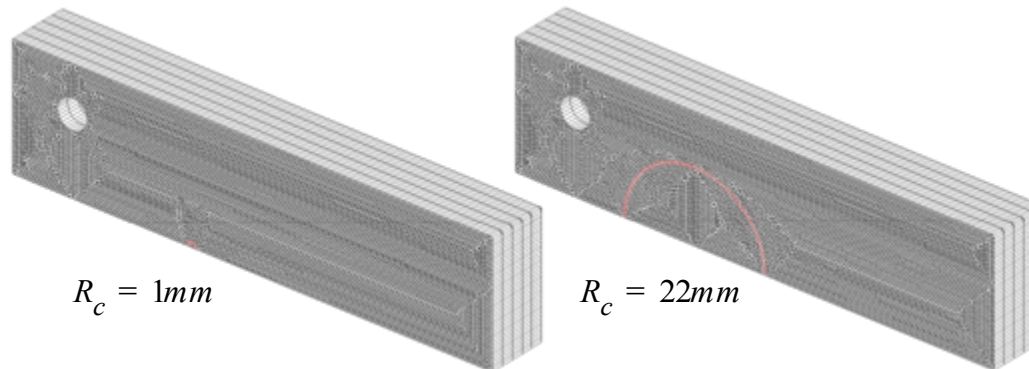
- Elastic isotropic
- Thickness =20 mm
- Linear crack front line
- $E = 210MPa$, $\nu = 0,3$



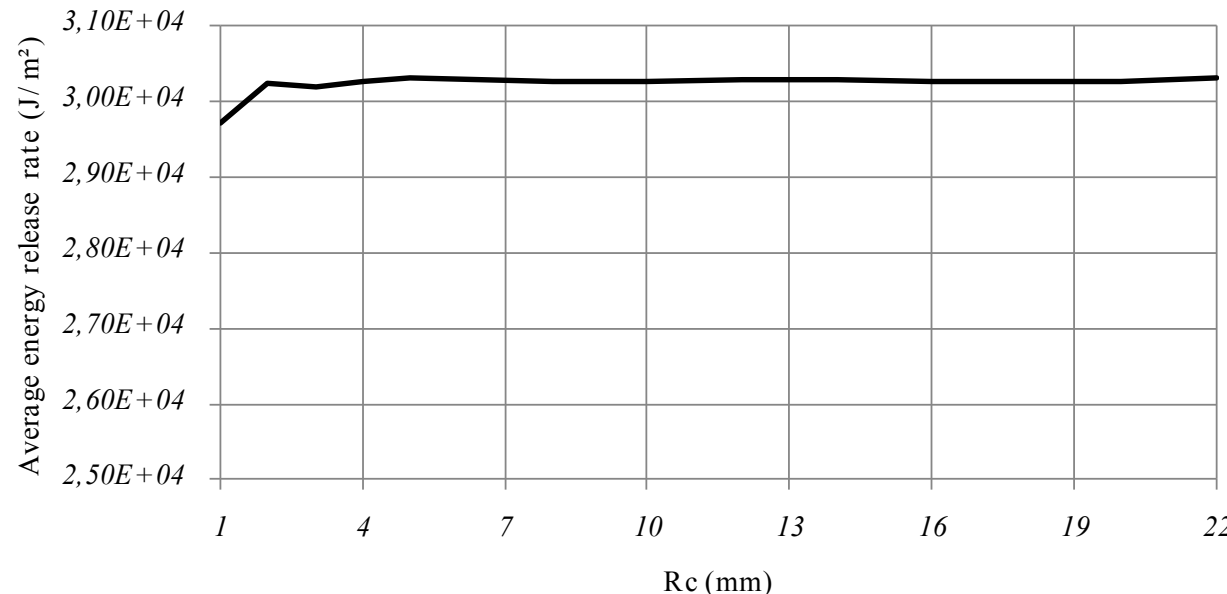
Algorithm for crack growth process



Numerical validation



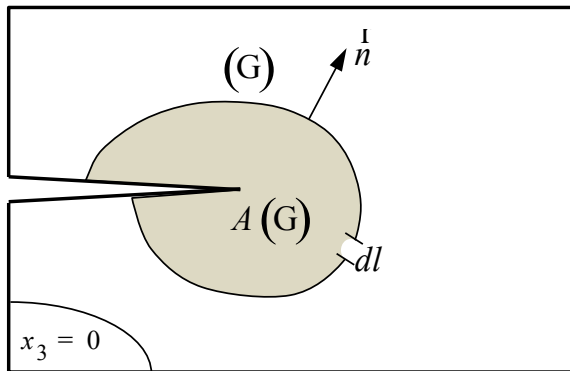
We can shows the variations of the energy release rate versus R_c :



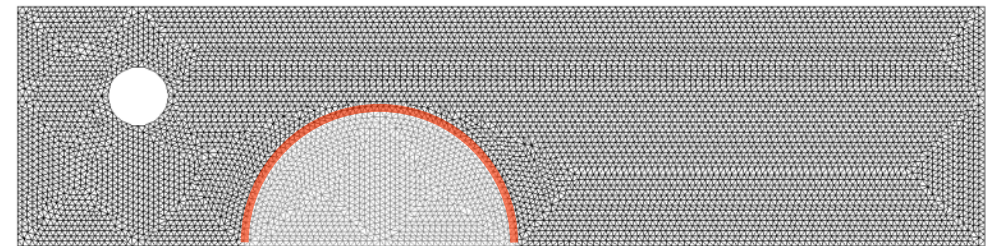
Numerical results validate the non-dependence of the integration domain with an average value of 30.3kJ/m²

Surface integration domains for the Bui's integral :

$$J_{Am} = \underbrace{\int_{\Gamma} (W \cdot n_1 - (\sigma_{ij} \cdot n_j \cdot u_{i,1})) \cdot d\Gamma}_{J^{2D}} - \int_{A(\Gamma)} \frac{d}{dx_3} (\sigma_{i3} \cdot u_{i,1}) \cdot dA(\Gamma)$$



Integration domains

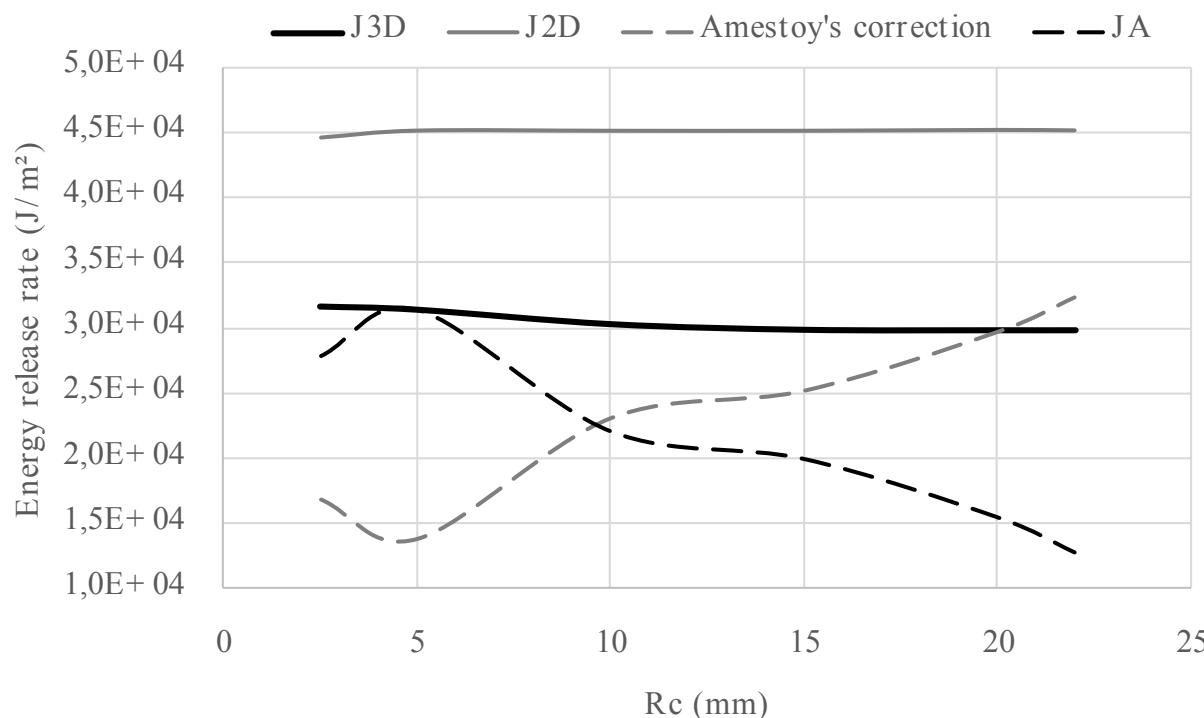


Integration domain size for 2D model

Physical interpretation

Surface integration domains for the Bui's integral :

$$J_{Am} = \underbrace{\int_{\Gamma} (W \cdot n_1 - (\sigma_{ij} \cdot n_j \cdot u_{i,1})) \cdot d\Gamma}_{J^{2D}} - \int_{A(\Gamma)} \frac{d}{dx_3} (\sigma_{i3} \cdot u_{i,1}) \cdot dA(\Gamma)$$

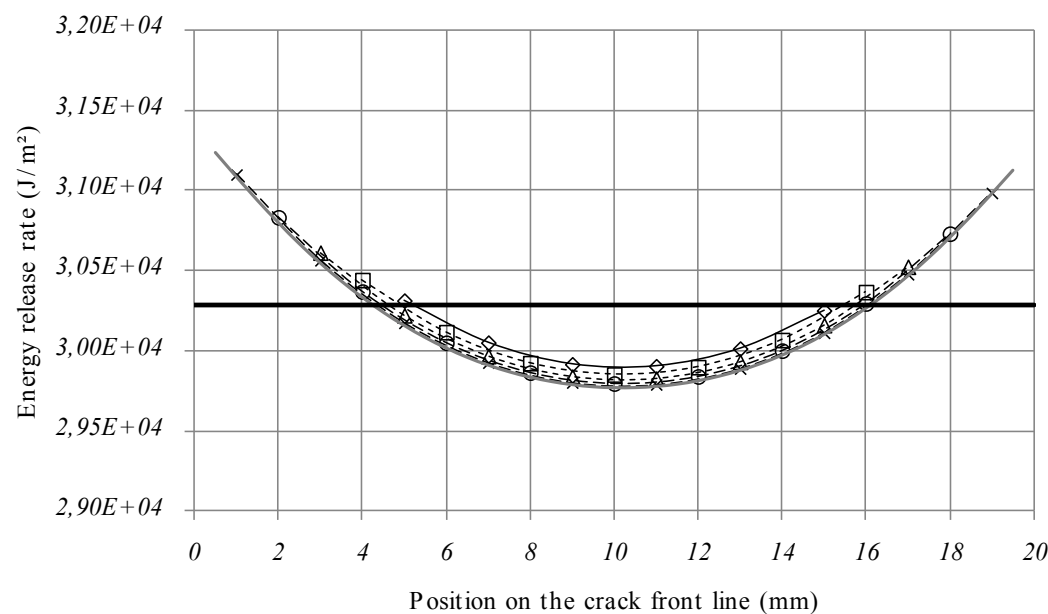
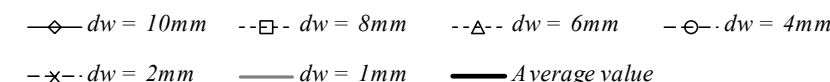
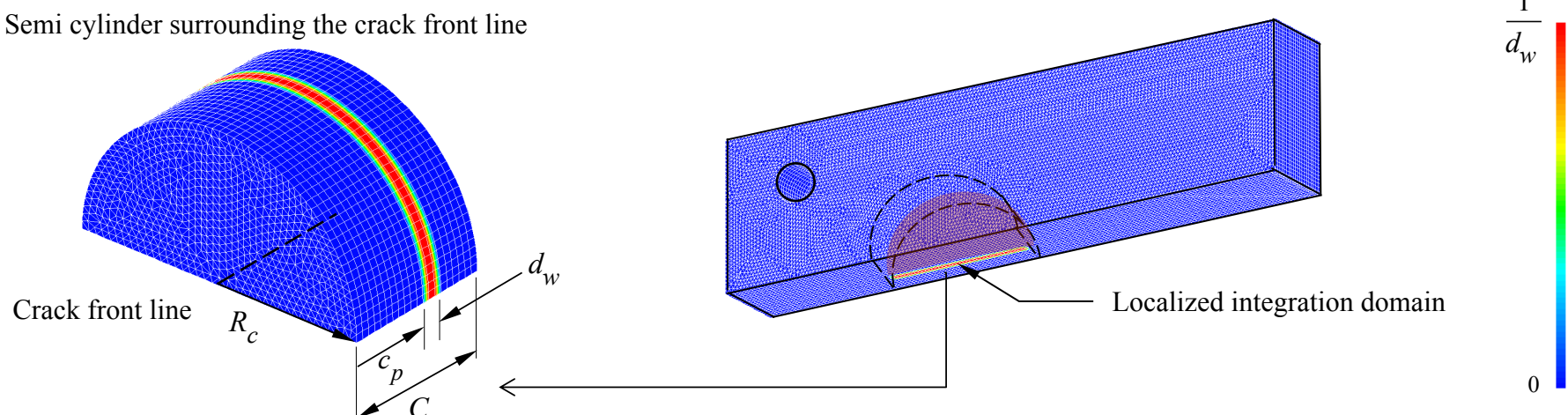


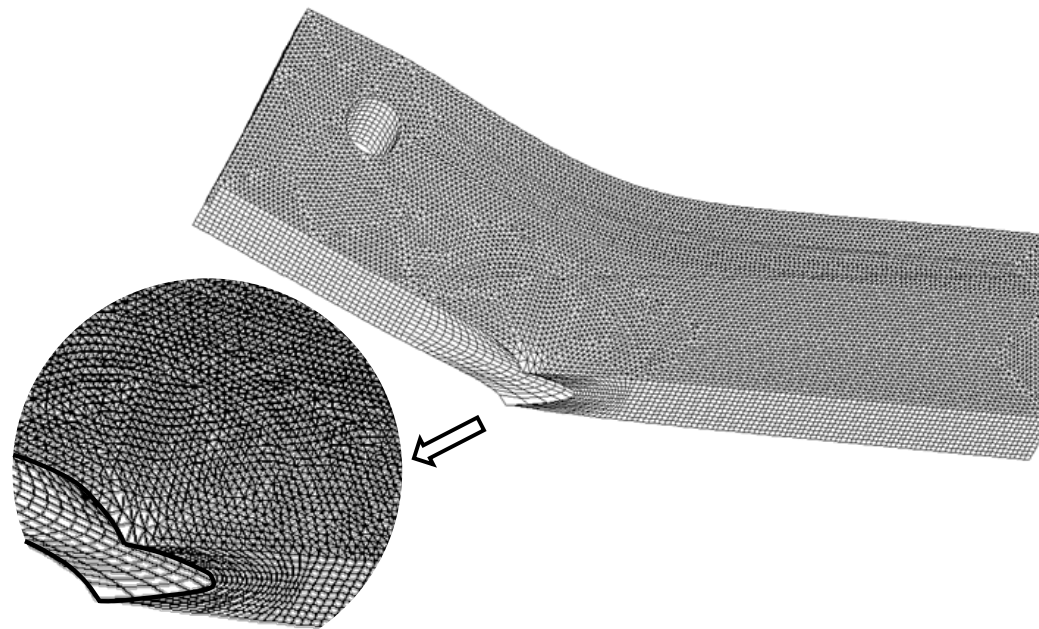
Comparison between J^{2D} and J^{3D} approaches



Numerical validation

Semi cylinder surrounding the crack front line



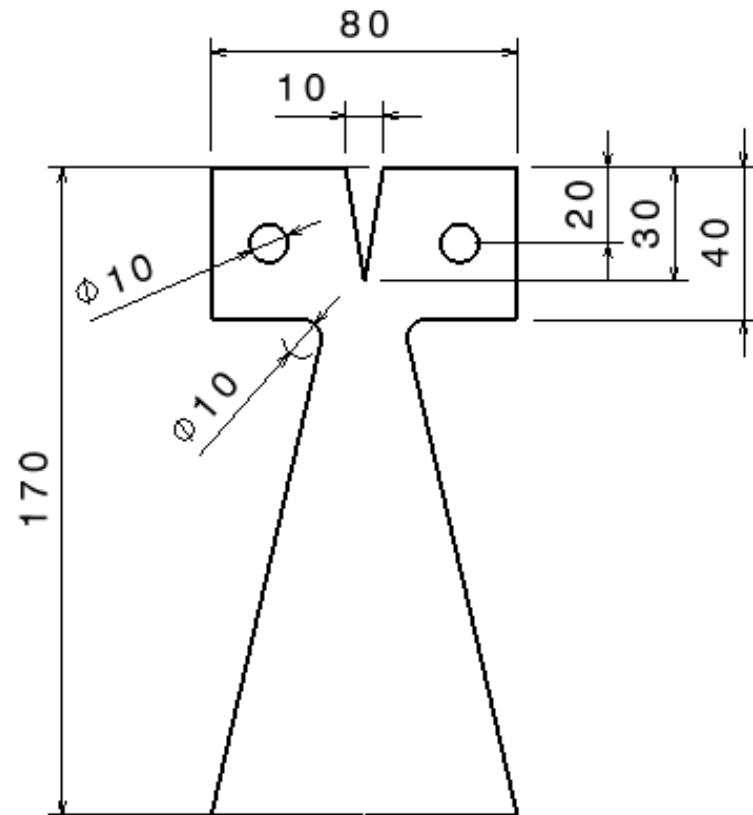
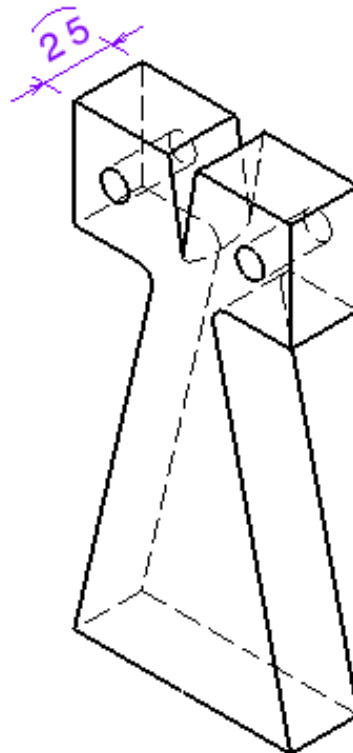


Crack front line

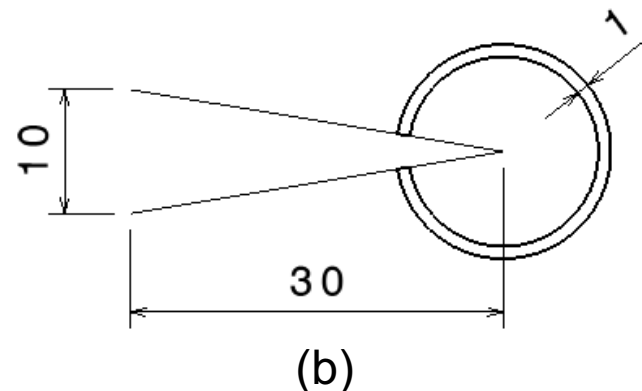
Layer	Average crack length (mm)	J^{3D}	J^{2D}	JA
1	61.8	42394	37646	30065
2	65	21687	31710	22148
3	67.4	14523	28034	19118
4	69	12025	25835	17417
5	69.8	11041	24835	16673

Numerical validation

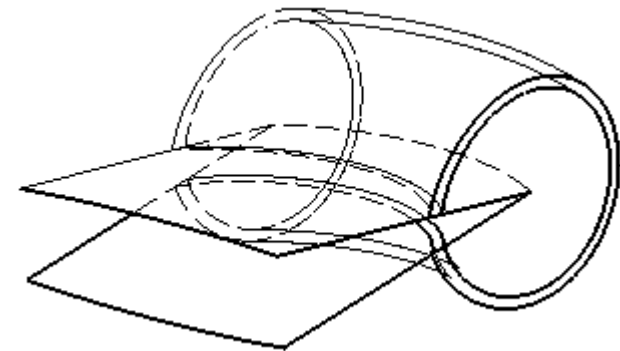
Using CAD software we can define our specimen as :



(a)



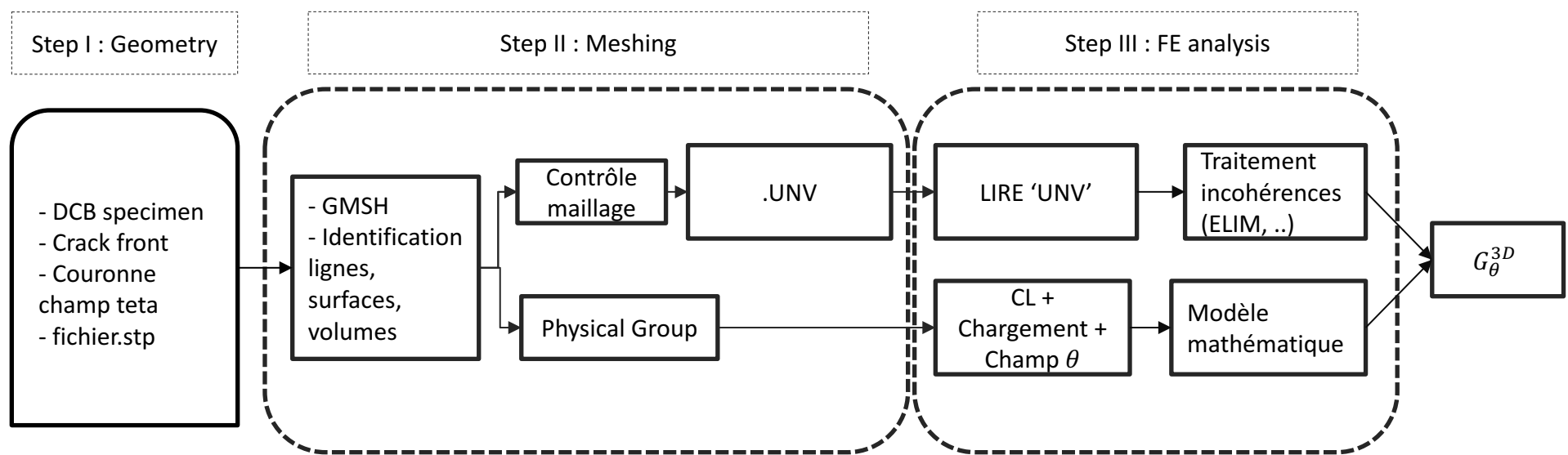
(b)



(c)

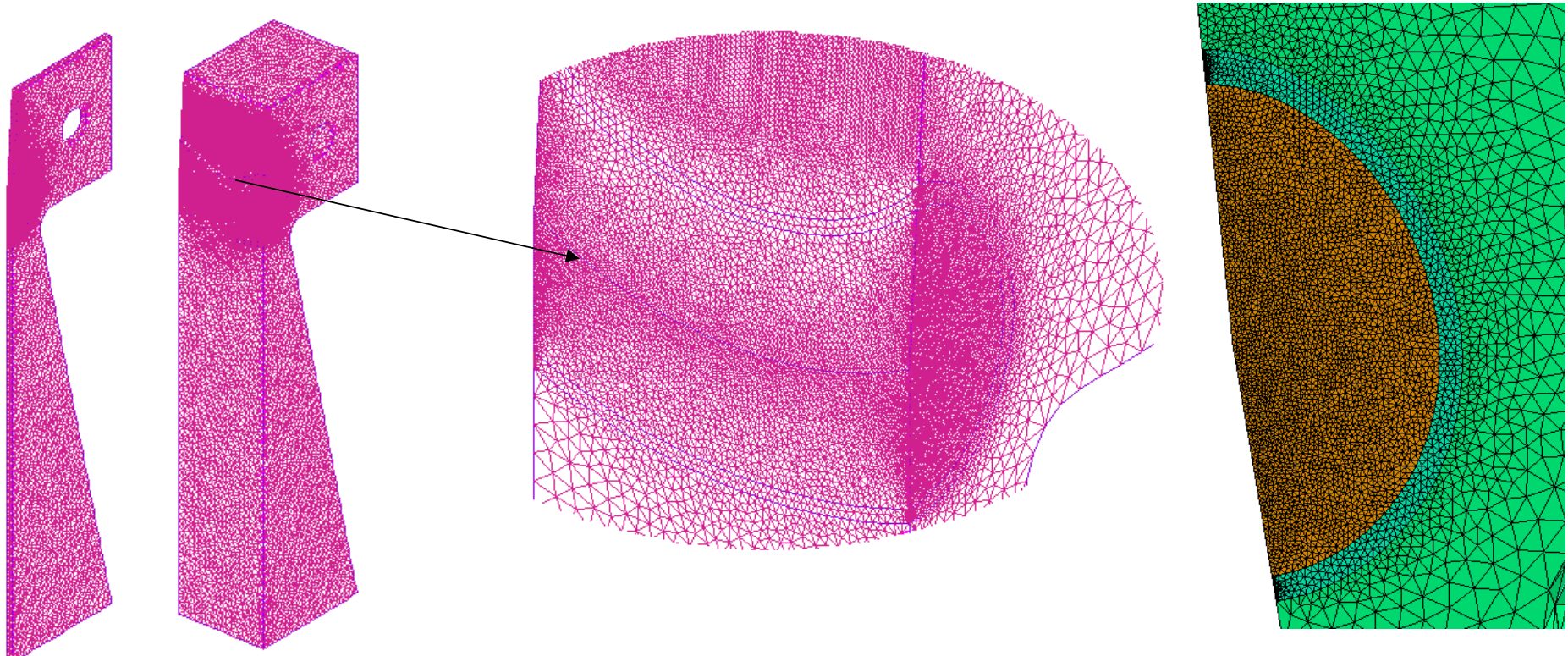
DCBVI specimen (a), two dimensional crack tip (b)
and three-dimensional elliptical crack front (c)

Algorithm for crack growth process



Post traitement :

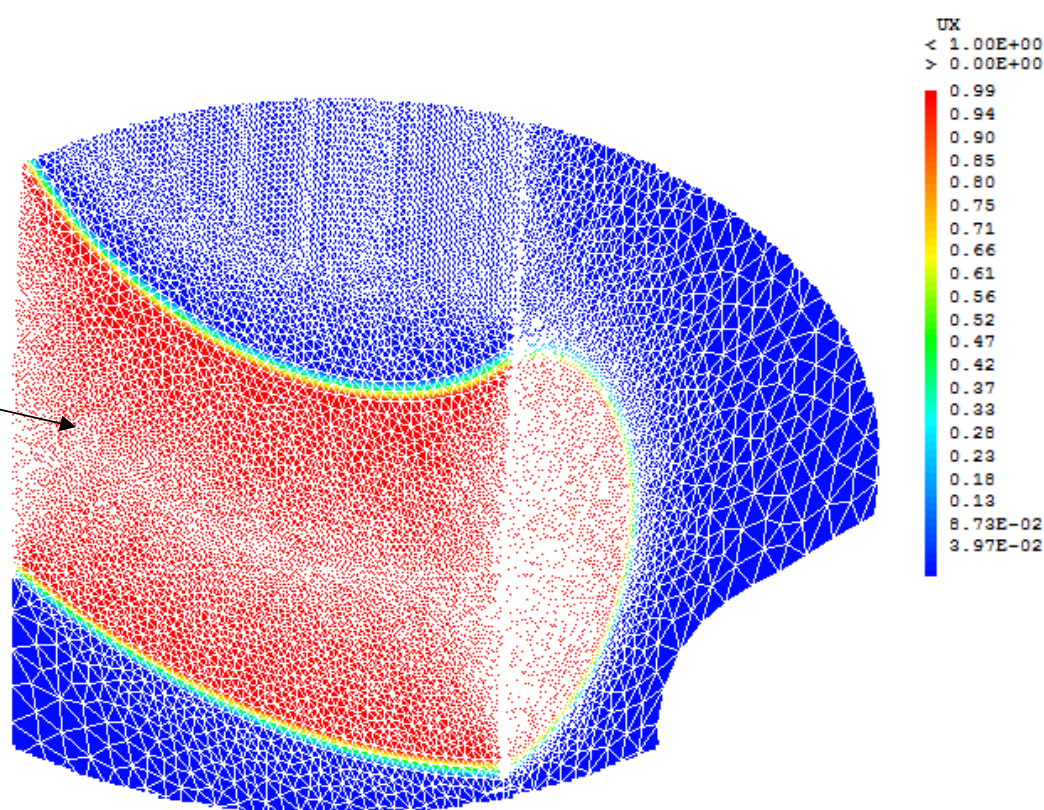
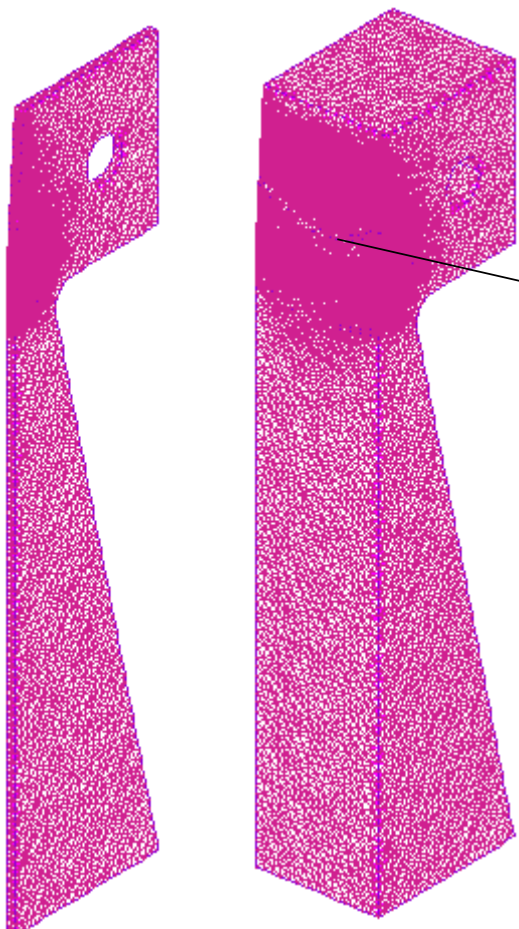
- ✓ Calcul de G à partir du l'intégrale $G_{\text{teta}}\text{-}3D$
- ✓ Vérification de l' indépendance du chemin d'intégration
- ✓ Tracer l'évolution de K1 le long du cfl
- ✓ ...



DCB Mesh with theta field : Typical FE meshes of the $\frac{1}{2}$ half DCBVI specimen

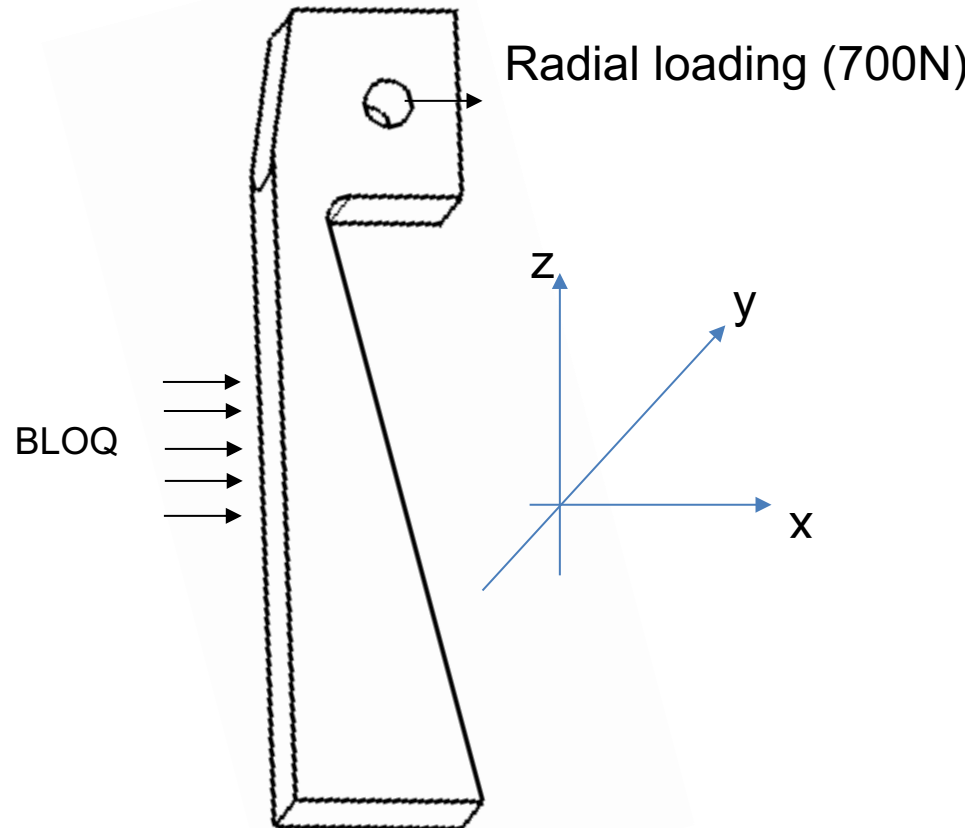


Numerical validation

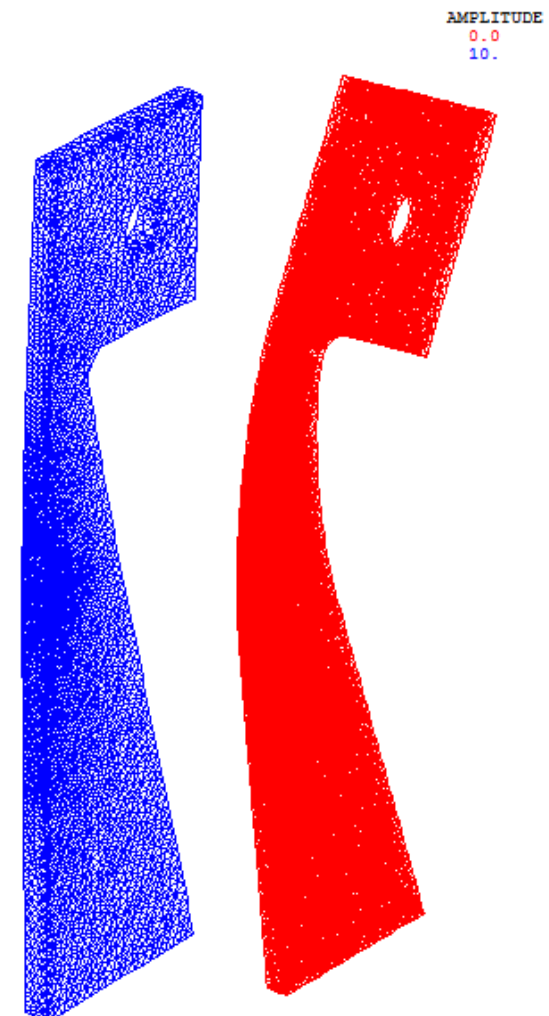




Numerical validation



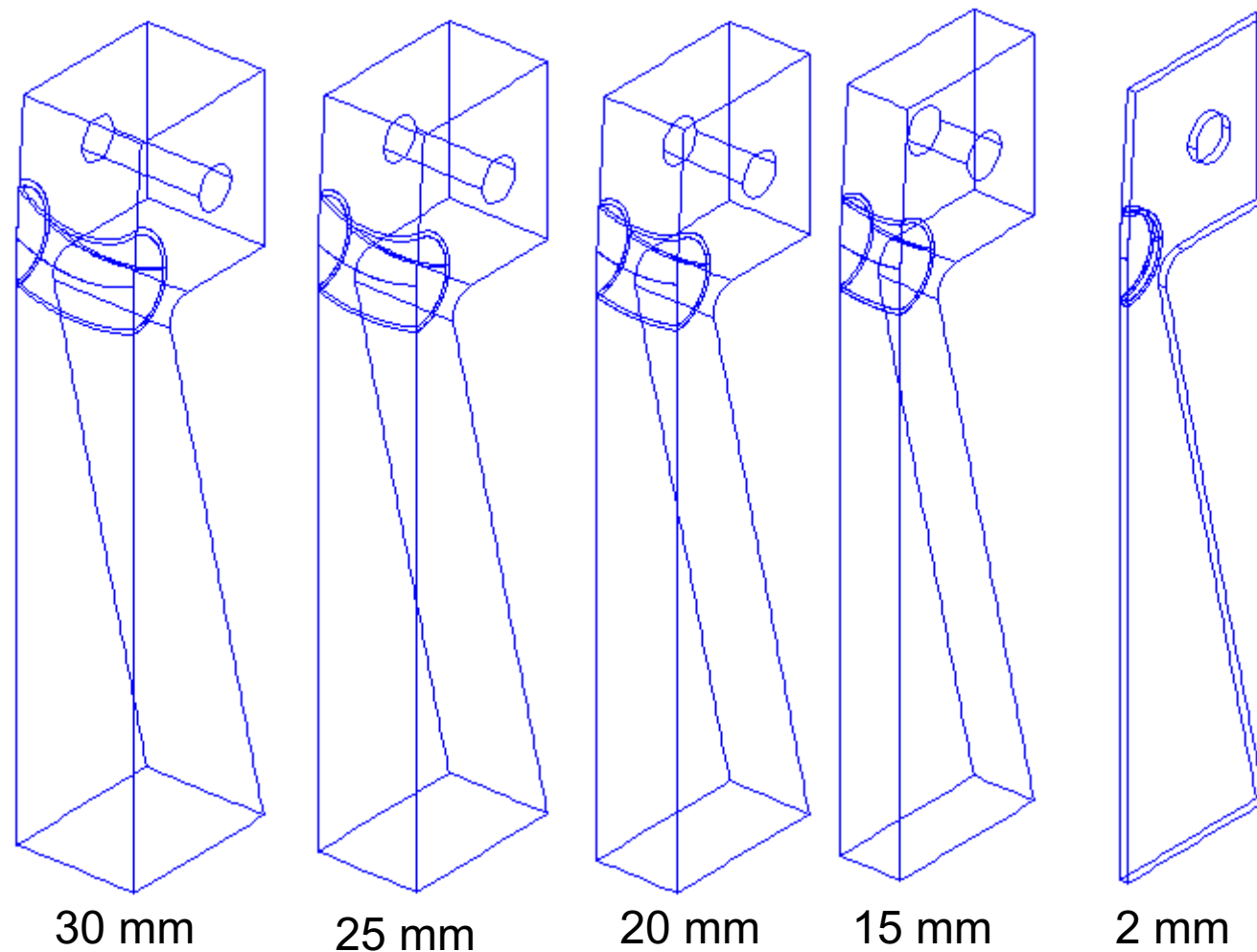
Boundary conditions



La déformée(Castem)



Numerical validation



Vue filaire des segments

- Scientific context
- Part I : three dimensional contour integral generalizations
 - Analytical formulation (J^{3D} and G_θ^{3D} -integral)
 - Numerical implementation
- Part II : mixed mode three dimensional contour integral
 - Analytical formulation (M_θ^{3D} -integral)
 - Mixed mode Numerical implementation
- Conclusions and outlooks



M^{3D} Integral

The M-integral formulation is based on the Noether's theorem application :

$$\delta L = \int_V \int_t \delta W \cdot dV \cdot dt = 0$$

A Gauss-Ostrogradski transformation allows us writing the Lagrangian's invariance in the form:

$$\begin{aligned} & \int_S \left(W^* \cdot n_k - \left(\frac{\partial W^*}{\partial u_{i,j}} \cdot n_j \cdot u_{i,k} \right) - \left(\frac{\partial W^*}{\partial v_{i,j}} \cdot n_j \cdot v_{i,k} \right) \right) \cdot dS \\ & + \int_V \left(\left(\frac{\partial W^*}{\partial u_{i,\alpha}} \cdot \delta u_{i,k} \right)_{,\alpha} + \left(\frac{\partial W^*}{\partial v_{i,\alpha}} \cdot \delta v_{i,k} \right)_{,\alpha} - W^*_{,k}(u) - W^*_{,k}(v) \right) \cdot dV = 0 \end{aligned}$$

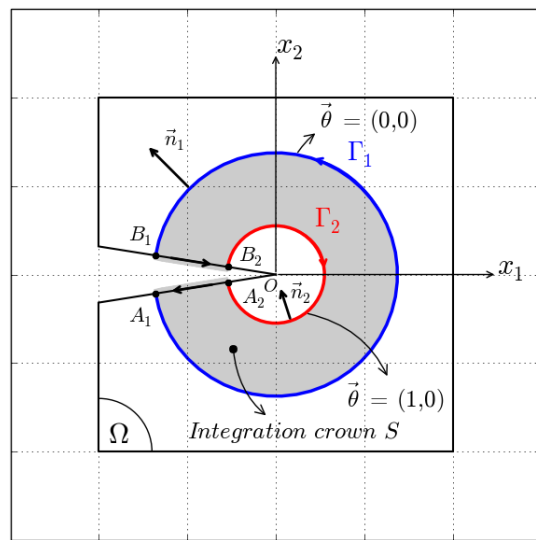
M^{3D}-integral

$$M^{3D} = \int_{S_{\Gamma_1}} \left(\sigma_{ij}^v \cdot u_{i,j} \cdot n_k - \frac{1}{2} (\sigma_{ij}^v \cdot u_{i,k} + \sigma_{ij}^u \cdot v_{i,k}) \cdot n_j \right) \cdot dS \quad \xleftarrow{①}$$

$$+ \int_{S_{CF}} \left(\sigma_{ij}^v \cdot u_{i,j} \cdot n_k - \frac{1}{2} (\sigma_{ij}^v \cdot u_{i,k} + \sigma_{ij}^u \cdot v_{i,k}) \cdot n_j \right) \cdot dS \quad \xleftarrow{②}$$

$$+ \frac{1}{2} \int_{V_{\Gamma_1}} \left(\left(\sigma_{ij}^v \cdot (\varepsilon_{ij}^u)_{,k} + \sigma_{ij}^u \cdot (\varepsilon_{ij}^v)_{,k} \right) - \left((\sigma_{ij}^v \cdot \varepsilon_{ij}^u)_{,k} + (\sigma_{ij}^u \cdot \varepsilon_{ij}^v)_{,k} \right) \right) \cdot dV \quad \xleftarrow{③}$$

M_θ^{3D} Integral



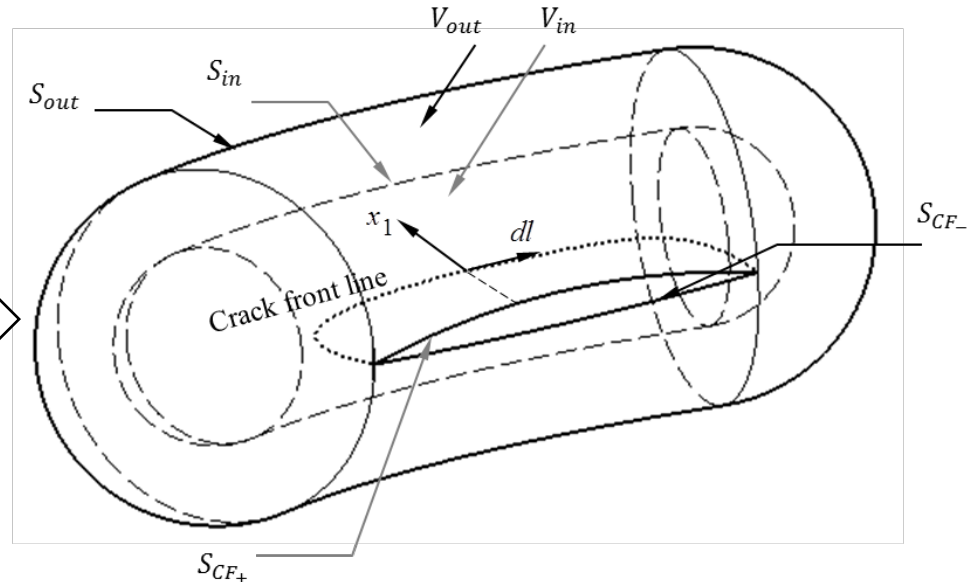
Integration domain size
for 2D

M_θ^{3D}-integral

$$M_{\theta}^{3D} = \frac{1}{2} \int_V P_{kj} \cdot \theta_{k,j} \cdot dV$$

$$- \frac{1}{2} \int_{S_{CF}} (\sigma_{ij}^v \cdot u_{i,k} + \sigma_{ij}^u \cdot v_{i,k}) \cdot n_j \cdot \theta_k \cdot dS$$

$$+ \frac{1}{2} \int_{V_{\Gamma_2}} \left((\sigma_{ij}^v \cdot (\varepsilon_{ij}^u)_{,k} + \sigma_{ij}^u \cdot (\varepsilon_{ij}^v)_{,k}) - \left((\sigma_{ij}^v \cdot \varepsilon_{ij}^u)_{,k} + (\sigma_{ij}^u \cdot \varepsilon_{ij}^v)_{,k} \right) \right) \cdot \theta_k \cdot dV$$



3D Closed volume and
surfaces integration
domains

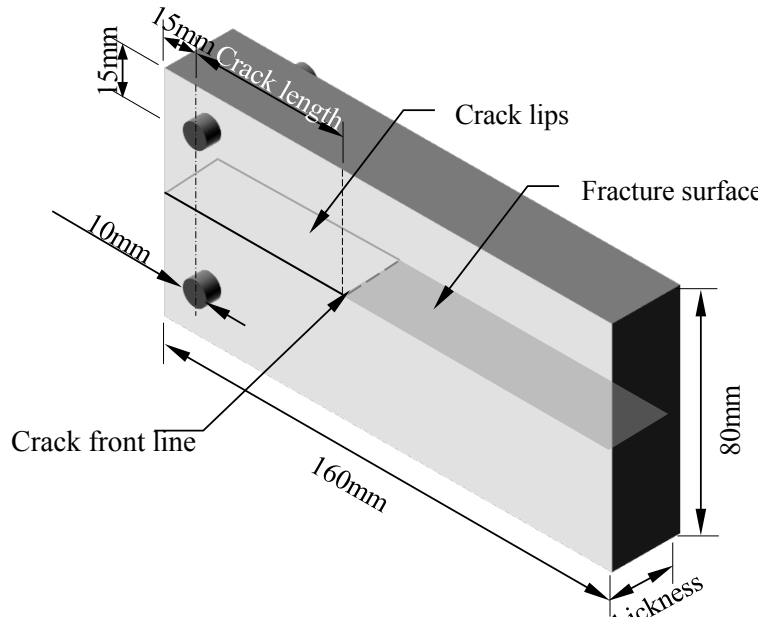
①

②

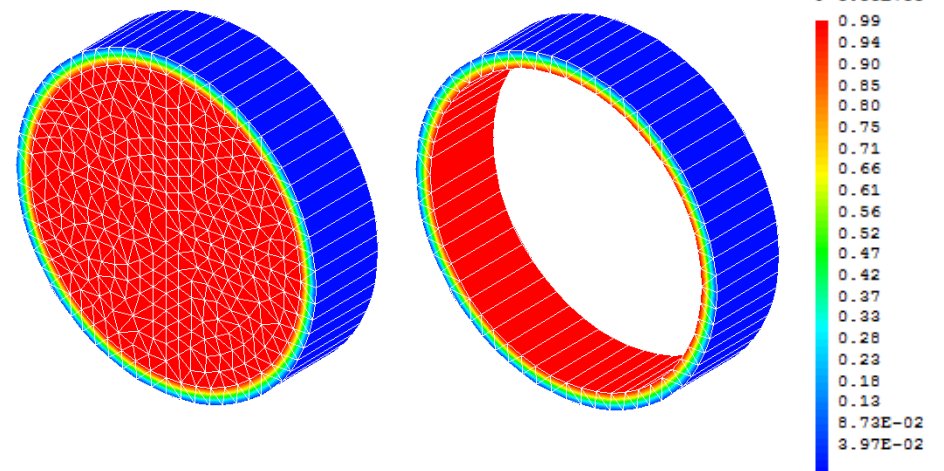
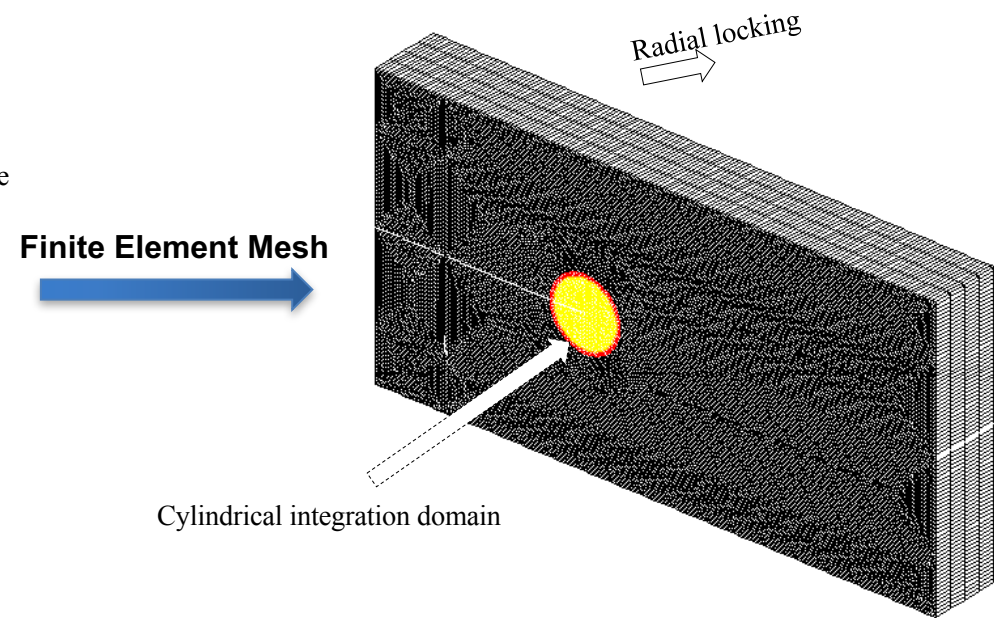
③

Numerical validation

The finite element implementation is based on a Double Cantilever Beam loaded in an open mode.

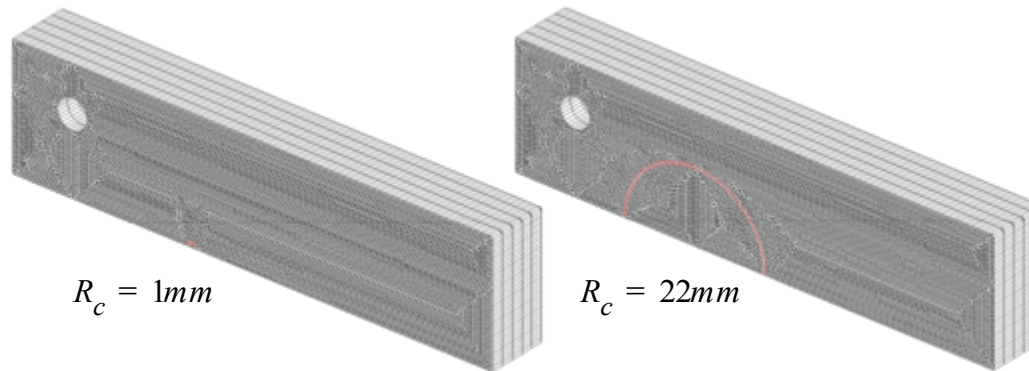


Specimen DCB

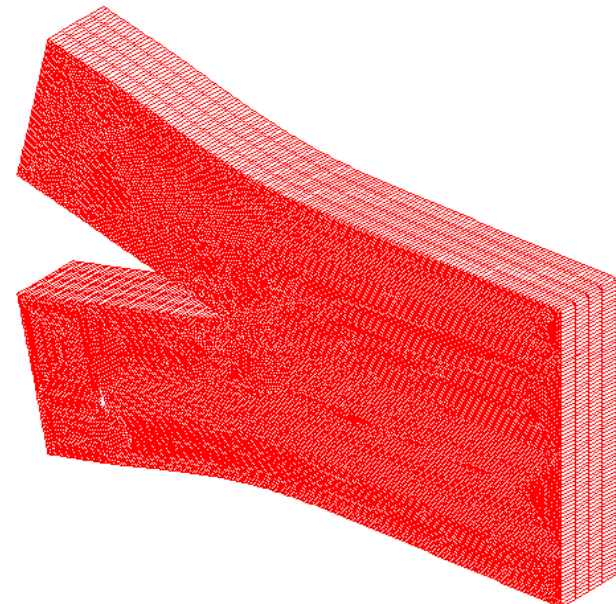
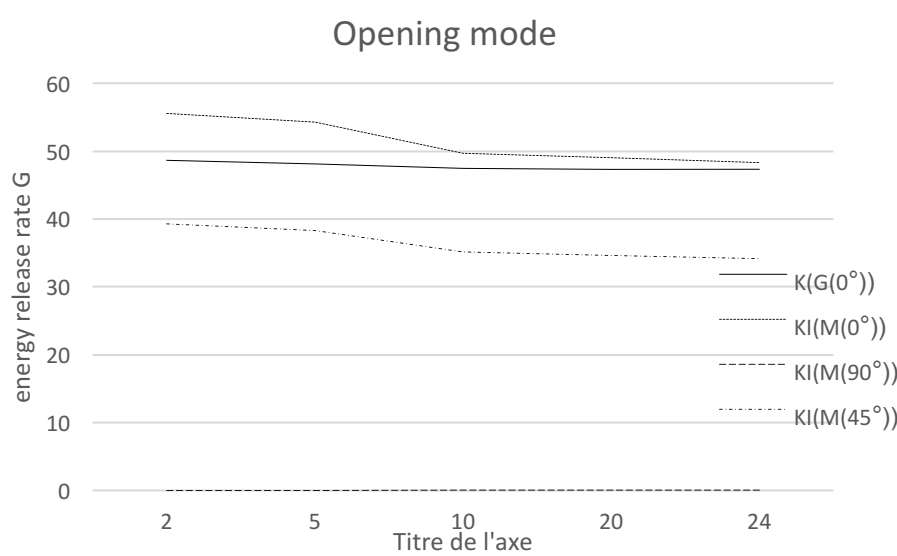




Numerical validation



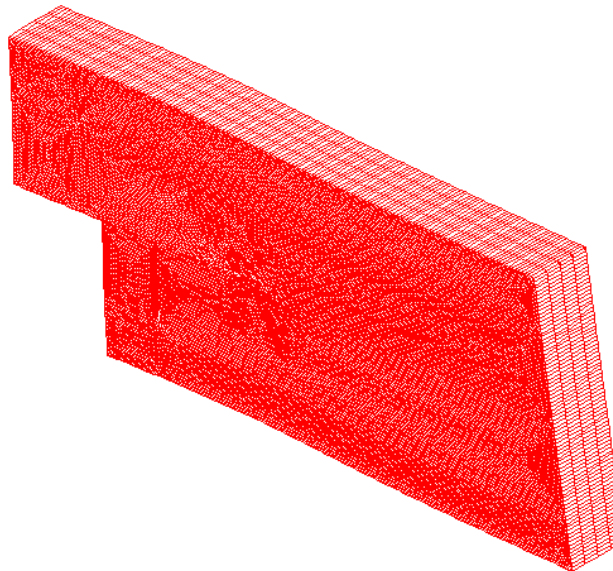
We can shows the variations of the energy release rate versus R_c :



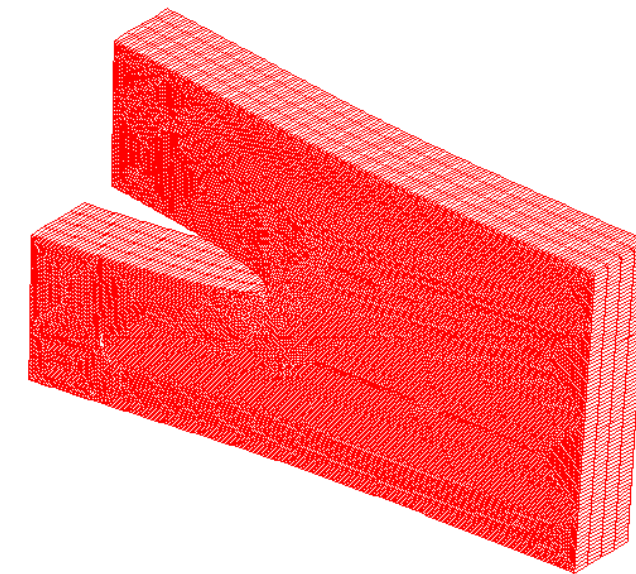
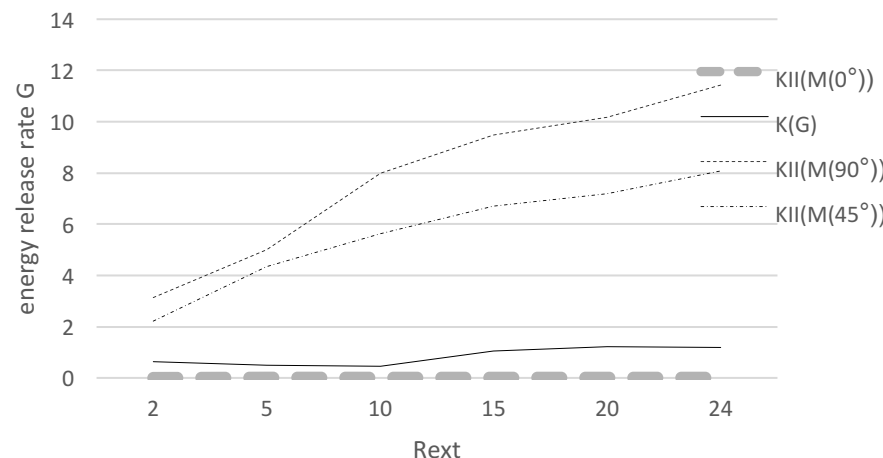
Numerical results validate the non-dependence of the integration domain with an average value.



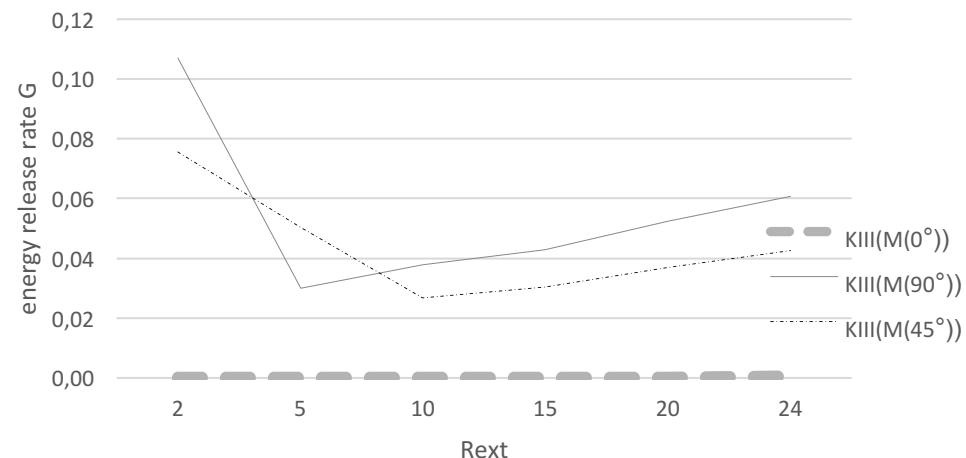
Numerical validation



Shear mode



out-of-plan shear mode



Numerical results validate the non-dependence of the integration domain with an average value.

- Numerical development of the contour integral concept for 3D problems
 - The generalization toward its G_θ^{3D} and M_θ^{3D} implementation form
 - Several numerical applications are proposed
 - Toward implementation three dimensional mixed mode crack problem
 - Elliptical crack front
-
- Numerical development of the contour integral concept for 3D problems.
 - Generalization of the local mechanical fields
 - New integral taking into account climatic effect
 - 3D fractures coupling hygrothermal with mechanics effects
 - Coupled 3D fracture mechanic – probabilistic methodology
 - Confrontation FE / Experimental results